Compensating focusing for space hyper spectral imager's fore optical system

Yicha Zhang (张益茬)[1,2*] and Wei Liu (刘 伟)[1]

[1] *Changchun Institute of Optics, Fine Mechanics and Physics, Chinese Academy of Sciences, Changchun 130033, China*

[2] *Graduate University of the Chinese Academy of Sciences, Beijing 100049, China*

[*] *Corresponding author: zhych6998@163.com*

Received August 12, 2010; accepted September 21, 2010; posted online January 28, 2011

The performance of space hyper spectral imager is severely affected by turbulent orbit temperature. Turbulence results in a defocus in the fore optical system of the imager. To address this problem, a focusing system is added. A number of simulation methods are applied on the fore optical system to study the relationship between temperature and focusing. In addition, this process is conducted to obtain a practical reference for focusing while the imager is flying on orbit. The obtained correlation between focusing and temperature is proven effective based on ground imaging and simulation testing.

OCIS codes: 110.6770, 350.6090, 230.4685.

doi: 10.3788/COL201109.021102.

The hyper spectral imager, a novel type of remote sensor, comprises several spectrometers and a fore optical system, of which the main element is an off-axis reflective telescope. The performance of the imager is largely dependent on the telescope system. Temperature turbulence[1,2] in the space environment causes deformation of the mirrors and the imager structure, especially the fore optical system. Deformation directly causes surface deviation and relative movement of mirrors, which then induces defocusing and the overall degradation of imager performance; it can even cause the imager to stop working. To address this problem, a compensating focusing system has been developed and placed on the imager. However, ensuring compensating focusing when the imager encounters different temperatures remains unclear. It is not practical to guess by engineering experience or grope blindly while the sensor is flying on orbit, which is unreliable and time-consuming. As it is necessary to clarify the relationship between focusing and temperature, exploring credible references for imager focusing is discussed in this letter.

The presently developed hyper spectral imager could gather spectral information by using its 128 spectral channels. The imager was with a focal length of more than 1000 mm, spectral resolution of 10 nm within the range of 0.4–2.5 μm, and spatial resolution of 0.025 mrad. The fore optical system of the imager comprised three sub-systems: pointing system, off-axis telescope system, and focusing system. The fore optical system is shown in Fig. 1.

Both pointing and focusing mirrors were mobile, whereas the other three reflective mirrors of the telescope were strictly fixed on the main structure. The pointing mirror was directed to ground objects and to collect parallel light. The focusing mirror was used to compensate the defocusing. If all mirrors, except the pointing mirror, would move or rotate, the image of the optical system would deviate from the focal plane placed behind the focusing mirror. Generally, this mechanism is caused by the thermal elastic deformation of the structure and mirrors, given the existing differences in temperature. However, the pointing system was not considered in this letter because of its limited contribution to the focus of our study. The main frame, mirrors, and supporting parts were studied primarily. The simplified mechanical system is shown in Fig. 2.

Based on thermal elasticity theory, a thermal-elastic simulating model[3−6] can be built using the finite element method (FEM). The model was used to simulate the thermal response of the fore optical system under different temperatures. In accordance with the basic fundamental of elasticity, some assumptions and simplifications were employed to simplify the equation solving. Reforming the physical equation of common elasticity was necessary in considering the effect of temperature difference. The reformed physical equation[7] is

$$\left.\begin{aligned}
\varepsilon_{xx} &= \frac{1}{E}[\sigma_{xx} - \mu(\sigma_{yy} + \sigma_{zz})] + \alpha_T \cdot \Delta T \\
\varepsilon_{yy} &= \frac{1}{E}[\sigma_{yy} - \mu(\sigma_{xx} + \sigma_{zz})] + \alpha_T \cdot \Delta T \\
\varepsilon_{zz} &= \frac{1}{E}[\sigma_{zz} - \mu(\sigma_{xx} + \sigma_{yy})] + \alpha_T \cdot \Delta T \\
\gamma_{xy} &= \frac{1}{G}\tau_{xy}, \gamma_{yz} = \frac{1}{G}\tau_{yz}, \gamma_{zx} = \frac{1}{G}\tau_{zx}
\end{aligned}\right\}, \quad (1)$$

where $\varepsilon_{i,j}$ and $\gamma_{i,j}(i,\ j = x, y, z)$ are strain components; $\sigma_{i,j}$ and $\tau_{i,j}$ are stress components; $G = E/[2(1+\nu)]$, E is the Young's modulus, ν is the Poisson ratio; ΔT is the temperature difference relative to the reference tempera-

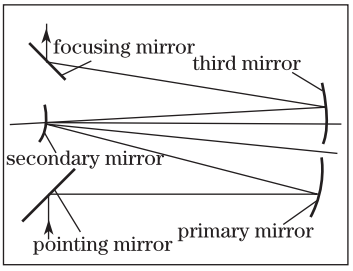

Fig. 1. Schematic of the fore optical system.

ture; and α_T is the thermal expansion coefficient. A calculation model solving deformation and thermal stress of the fore optical system was built from the FEM software platform, MSC.patran, as shown in Fig. 3.

In general, the temperature of space capsules changes from –10 to 45 °C while flying in earth orbit. In contrast, the ideal working temperature of the imaging system (i.e., assembling temperature; all mirrors placed at the ideal positions) is 18 °C. In a system, thermal controlling devices can only ensure working temperature fluctuating at ± 10 °C.

In the FEM model, the reference temperature was set to 18 °C, with the lowest temperature at 8 °C and the highest at 28 °C. A group of discrete temperature loads was applied on the model separately. Corresponding thermal deformation and thermal stress results were obtained individually after calculation. Results of the experiment are shown in Figs. 4–7.

Based on deformation results, the mirrors and structure would deform differently at various temperatures, subsequently causing deviation, translation, and rotation of the mirror surfaces. Thereafter, defocusing would occur. After simulation, the deformation results extracted from the FEM model were processed by Zernike polynomial in order to obtain the interface between mechanical data and optical data. The processed data were then

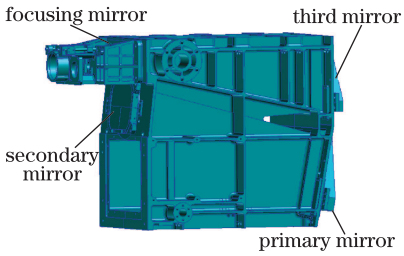

Fig. 2. Schematic of the mechanical structure.

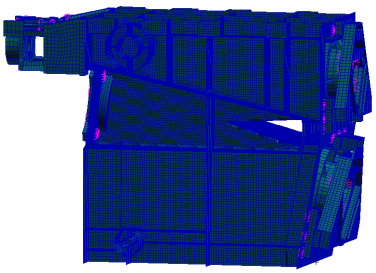

Fig. 3. FEM model of the fore optical system.

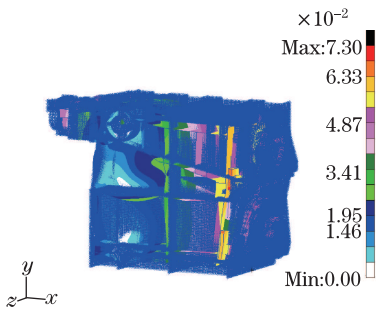

Fig. 4. Deformation at 8 °C (shrinkage) of the main frame.

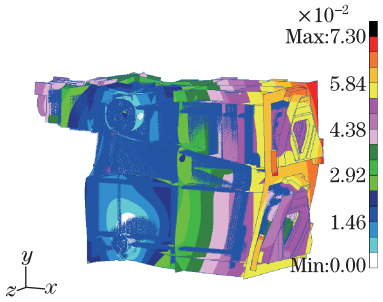

Fig. 5. Deformation at 28 °C (expansion) of the main frame.

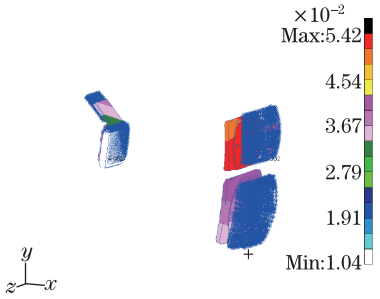

Fig. 6. Mirror deformation at 8 °C (shrinkage).

Table 1. Defocusing Amounts under Different Temperatures (Flying Direction is Negative)

Temperature (°C)	Defocusing Amount (μm)
8	−176.6
10	−132.4
12	−98.6
14	−63.5
16	−27.8
18	0
20	28.4
22	63. 8
24	102.2
26	135.8
28	179.2

entered into the optical system using an optical design software platform, Code-V. The defocusing values for the fore optical system at different temperatures were analyzed. The predicted correlation between defocusing amount and temperature is presented in Table 1.

Table 1 shows that the largest defocusing amount is nearly up to ± 180 μm, which exceeds the limit of the focal depth of the spectral imager. The focal depth is expressed as[8]

$$|\pm\Delta| = 2F^2\lambda, \tag{2}$$

where F is the F number and λ is the central wavelength of the spectral range collected by the spectral imager. The focal depth of the fore optical system is

$$\Delta = \pm 2F^2\lambda = \pm 2 \times 5.54^2 \times 0.6328\,\mu\text{m} = \pm 38.8\,\mu m.$$

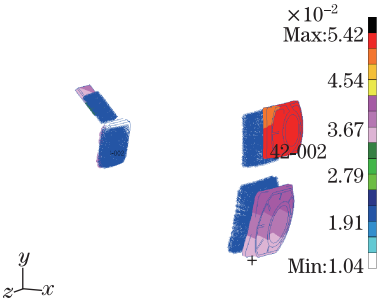

Fig. 7. Mirror deformation at 28 °C (expansion).

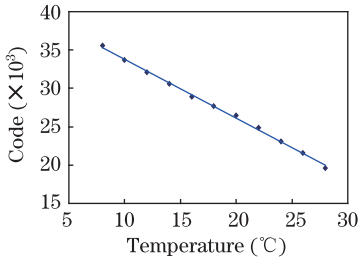

Fig. 8. Relation between focusing amount and temperature (FEM results).

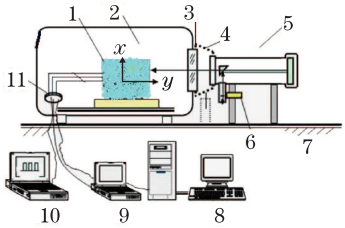

Fig. 9. Experimental apparatus. 1: space imager; 2: vacuum tank; 3: light window; 4: shielding cover; 5: collimator; 6: target board/monochromator/light sources; 7: air-floating platform; 8: temperature controller/tester; 9: simulation instrument; 10: quick image catcher; 11: plug.

Simulation results have predicted that when the temperature difference is larger than 3 °C, the excessive defocusing amount would degrade the spectral imager performance or even cause the imager to stop working at some temperatures. Therefore, it was inevitable for us to carry out compensation for defocusing. The defocusing amount could be used as a guideline for focusing. After amendments, the relationship between defocusing and temperature was determined and later transferred into the relationship between focusing amount and temperature, as shown in Fig. 8. After all mirrors were placed in their ideal positions, the coder of the focusing system displayed an expected value of 27700. Through translation, the focusing amount was linked to a code, which could then be used directly in practice, as shown in the equation below:

$$D = -769.33T + 41499, \tag{3}$$

where D is the code and T is the temperature.

A number of simulating experiments were carried out to explore the expected reliable relationship between focusing amount and temperature. The experiment was used to simulate space environment and to study the thermal responses of the fore optical system. The spectral imager

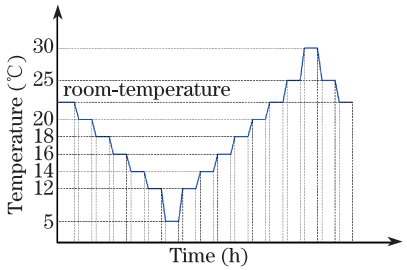

Fig. 10. Experimental load cases.

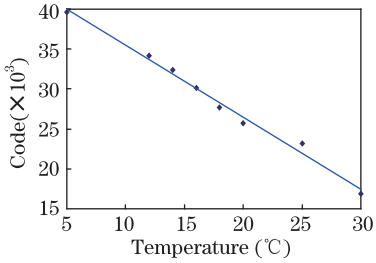

Fig. 11. Correlation between focusing amount and temperature (experimental results).

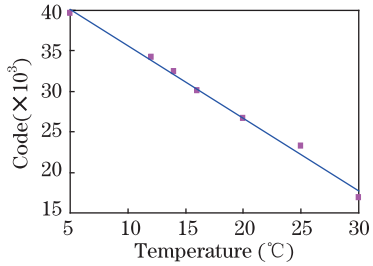

Fig. 12. Relation between focusing amount and temperature (final results).

was set in a big vacuous pot. The temperature in the pot was controlled by a device. A number of control and testing equipments were linked to the spectral imager by cables. The experimental apparatus is shown in Fig. 9.

After setting up all the apparatuses, the spectral imager was launched under different temperatures. The different testing apparatuses were activated separately. The temperature in the pot was nearly uniform during the whole testing process. The temperature loads in the experiments are presented in Fig. 10.

The theoretical simulation results, which could offer correct defocusing trending, enabled us to determine easily the best focal plane under certain temperatures. The results of the experiments also (Fig. 11) proved that the theoretical FEM model was both worthy and reliable. The testing results were then refined and transferred into the expected format to facilitate comparison with theoretical simulation results. The experimental results are expressed as

$$D = -901.35T + 44510. \tag{4}$$

To validate the simulation results, the spectral imager was placed in a space-simulating environment station in order to collect spectral message of a target placed some miles away and under different temperatures. These results were used to simultaneously conduct focusing and

imaging. The clear spectral images indicate that the predicted compensating focusing amount for the imager is practical; that is, the simulation results are reliable. The test agreed well with simulation results. The final results are shown in Fig. 12 and can be expressed as

$$D = -895.04T + 44612. \quad (5)$$

In this letter, the relationship between focusing amount and temperature is explored. The corresponding results can be used as a guide for space hyper spectral imager focusing. Both simulation and imaging tests have shown that temperature turbulence is the main factor inducing defocusing. When temperature rises or decreases, the image of the fore optical system deviates from the expected focal plane. The relationship between defocusing (or focusing amount) and temperature difference is approximately linear.

This work was supported by the National Defense Pre-Research Foundation of China under Grant No. O5001SA050. We express our appreciation to all who offered their help during the research.

References

1. P. R. Yoder, Jr., *Opto-Mechanical Systems Design* (3rd edn.) (SPIE Press, Bellingham, 2004).
2. H. Wang and C. Han, Opt. Tech. (in Chinese) **29,** 452 (2003).
3. G. Stoeckel, D. Crompton, and G. Perron, Proc. SPIE **6675,** 66750D (2007).
4. F. Li, P. Ruan, X. Ma, and B. Zhao, J. App. Opt. (in Chinese) **28,** 38 (2007).
5. Z. Li, Q. Wu, M. Gao, D. Dong, and C. Yan, Infrared Laser Eng. (in Chinese) **37,** (suppl.) 98 (2008).
6. W. Liu, Chin. J. Opt. App. Opt. (in Chinese) **13,** 157 (2010).
7. P. Zeng, *Finite Element Analysis and Application* (in Chinese) (Tsinghua University Press, Beijing, 2004).
8. Z. Wang, L. Zhang, C. Li, and X. Xun, Opt. Precision Eng. (in Chinese) **17,** 1051 (2009).